MECHANICS

UDC 539.219.1 https://doi.org/10.23947/1992-5980-2020-20-2-125-136

Investigation of crack propagation in the surface white layer of rail steel

A. Yu. Perelygina, V. Yu. Konyukhov, A. E. Balanovskii
Irkutsk National Research Technical University (Irkutsk, Russian Federation)

Introduction. The paper is devoted to the evaluation of cracking of white layers formed on the surface of the rail while in operation. Cracks are detected in the white layer of rail steel after one thousand test cycles. This is due to tensile and shear stresses on the surface of the wheel–rail contact spot. The paper presents the study results of the morphological characteristics of the white layer on the rail surface.

Materials and Methods. The object of study (rail surface after operation) was examined under a microscope. Then, a two-dimensional model of finite elements of the plane deformation was developed to simulate the dynamic characteristics of the white layer cracking. Mathematical models describing crack propagation are proposed. For this, we applied the criterion of the elastic plastic fracture mechanics, the *J*-integral method. The *SYSWELD* program performed numerical modeling of the formation of a white layer and the distribution of residual stresses.

Results. Optical images of the microstructure of the cross section of a white layer on the rail surface after operation are presented. Two different types of cracks were fixed at the trailing edge of the white layer of the samples studied. The *SYSWELD* program visualized fragments of simulating the mechanism of the white layer formation with the distribution of residual stresses, compression, and tension. The calculation results show that the values of the *J*-integral for all three cracks slightly decrease if the crack length reaches 10–50 μm.

Discussion and Conclusions. The results obtained are applicable to assess the wear resistance of rail steels and predict the direction of crack growth. Comparisons of *J*-integral maxima have shown that under identical load conditions, crack no. 1 is likely to grow faster than cracks nos. 2 and 3. With an increase in the length of the crack, the maxima of the *J*-integral of all three cracks decreased.

Keywords: rail steel, white layer, crack, elastic plastic fracture, *J*-integral method, distribution of residual stresses.

For citation: A. Yu. Perelygina, V. Yu. Konyukhov, A. E. Balanovskii. Investigation of crack propagation in the surface white layer of rail steel. Vestnik of DSTU, 2020, vol. 20, no. 2, pp. 125–136. https://doi.org/10.23947/1992-5980-2020-20-2-125-136

Introduction. It is known that parts of machines and mechanisms, various functional structures often experience catastrophic brittle fracture. Moreover, depending on the operating conditions, the metal may undergo plastic or brittle fracture [1-3]. Brittle fracture occurs due to the growth of cracks that suddenly become unstable and propagate in the material at sonic velocity. Cracks in the metal can be of technological origin or appear and grow during operation. White non-etching layer (*WEL*) is a phenomenon that occurs on the surface of an operated rail under the impact of wheels. *WEL* is formed due to strong multicycle plastic deformation. It has been established that due to fatigue from contact rolling on the rail surface, cracks bind to the white layer [4–6]. The layer is named because of its resistance to acid etching during metallographic preparation and the white "faceless" appearance (it looks like this under a microscope). A white layer is usually found in contact spots on the rail surface. Its depth is ~ 0.10–100 μm after several months of rail operation [4]. An important feature of the white layer is hardness. It reaches 1300 *HV* [5], but is usually in the range of 700–1200 *HV* [6]. This condition can cause the formation of brittle cracks in the white layer and subsequent propagation of fatigue cracks. The authors [4], having examined the rails after operation, found that cracks

were present in the white layer, but did not penetrate the interface with the base metal of the rail [4, 5]. Cracks developed on the surface and propagated along the interface between the *WEL* and the pearlite structure of the material causing severe wear. The mechanism of the formation of the white layer and its microstructure are studied by many authors [6–12].

The microstructure of the layer is identified as the following mixtures:

- martensite with residual austenite and pure martensite saturated with nitrogen and carbon;
- ferrite with martensite;
- residual austenite and martensite with tempered martensite;
- ferrite with cementite, carbide and nanocrystalline phase α-*Fe*.

It was found [6, 7, 9] that the white layer has a martensitic microstructure with a high dislocation density. The authors of [8–10] suggested that *WEL* consists of a nanocrystalline phase of α-*Fe* with grain sizes from 15 to 500 nm. According to [7], *WEL* consists of strongly deformed perlite, nanocrystalline martensite, austenite, and cementite. In [8], the results of X-ray measurements of residual compressive stresses in *WEL* are presented, and significant compressive stresses of the rail (~ 600 MPa) in both directions, longitudinal and transverse, are specified. An analysis of the papers [4–19] shows that cracks in the white layer of rail steel are detected after all tests, even those that were completed far just one thousand cycles. The reason for this is mixed tensile and shear stresses on the surface of the wheel – rail contact spot. After the appearance of a crack in the white layer, it grows rapidly due to the fragility of the martensite structure until it reaches the interface with the base metal of the rail having a perlite structure — here a different microstructure deflects the crack and slows its propagation. This deviation is caused by the orientation of the cementite plates in the pearlite structure [10–19], which are parallel to the rolling surface. According to [12], a decrease in rail fatigue resistance is associated with contact pressure and slip coefficient. The authors of [13] have found that the initiation of a crack in a white layer is caused by the traction force and the designed transverse shear load to the rail track surface. Two types of cracks are identified:

- leading defect crack in the contact spot (caused by a shift);
- back crack (brittle fracture in the form of a wedge).

The authors of [14] associated the short-wave dynamic interaction between the wheel and the rail with the beginning and growth of surface deformation. Under the conditions of contact rolling in rail steel under fatigue, three types of cracks were identified [15]:

1) perpendicular contact surfaces,
2) with a tilt angle,
3) parallel contact surfaces at various depths.

To determine the stress state near the crack tip under conditions of contact with rolling, the authors proposed a numerical method and recorded a change in the crack shape. In [16], the criteria for the direction of crack growth in the mixed mode were used to evaluate cracking behavior. It is shown that cracks grew in the direction of the plane of maximum shear stress, and not perpendicular to the plane. The authors of [17] developed a two-dimensional finite element model for simulating the crack behavior in the rolling contact (wheel and rail) with four short cracks. It was found that the shear stress plays a dominant role in the crack growth, a longer crack grows upward, and this causes a breakaway of the surface layer. Using a two-dimensional computational model, the authors of [18] found that the growth rate of cracks on the rail surface increases with increasing crack length and starts to decrease after a certain depth. In the study on the dynamic wheel and rail interaction [19], a three-dimensional model of finite elements was used and various cracking behavior was recorded due to the static and dynamic solutions. In [20], the residual stress effects were taken into account when studying the path and rate of crack growth. Many works including [21, 22] show the influence of a liquid on the further development of cracks. It is assumed that the liquid on the surfaces of the cracks significantly affects their opening (stress intensity factor of mode I). If the crack develops under dry conditions, then the

shear regime dominates [22]. Until now, linear mechanics of elastic fracture has been widely used under the numerical simulation of the contact of wheels and rails [23, 24]. This approach evaluates the resistance to unstable crack propagation, or the crack resistance of metals, under static loading according to one or more fracture criteria:

- force (critical stress intensity factor K_{1c});
- deformational (critical opening at the crack tip);
- energy (the critical value of the *J*-integral, the work of plastic deformation and fracture).

In practice, materials near the contact area can be plastically deformed due to the high axial load [3–6]. To obtain a more accurate solution, calculations using elastoplastic fracture mechanics or energy-based criteria should be used. In addition, cracks can be formed in areas adjacent to the white layer [7–12], and the mechanisms of their development are still not properly understood. Papers on the formation of a white layer and cracks [14, 15] are published; however, the behavior of the crack propagation in the area of the white layer is not studied in detail. Moreover, in relation to the situation under consideration, the impact of loading conditions, friction, and other interaction parameters is not described. This paper presents results of the study on the morphological characteristics of the white layer on the rail surface.

Materials and Methods. At first, the object of study was examined under a microscope. Then, a two-dimensional model of finite elements of plane deformation was developed to simulate the dynamic characteristics of cracking of the white layer. According to the hypothesis put forward, the contact area on the rail surface was plastically deformed under the interaction of the wheel and the rail; therefore, the energy-based *J*-integral criterion was introduced to evaluate the crack propagation behavior.

Samples containing white layers on the surface of the railhead were cut from the rail, which used to be operated on the East Siberian Railway. The rail was made of pearlite steel in accordance with GOST51685-2013. This is grade 76KhF steel: *C* 0.78%, *Si* 0.54% and *Mn* 0.8%, *Cr* 0.40%, *V* 0.035%. The mechanical properties of the rail were determined:

- yield strength was 944 kN,
- temporary resistance was 1287 kN,
- elongation was 11.5%,
- relative reduction was 31%,
- impact strength was 18 J/cm^2.

The test temperature was +20°C. Brinell macrohardness on the rolling surface in places without white layers was 435, 485, 445, 465 and 494. This does not meet the requirements of GOST 51685-2013 (should be 352–405 according to Brinell). Hardening of the railhead surface during operation is due to the combined action of a number of physical mechanisms [4–16]. For the calculation, the Young's modulus E = 206 GPa was adopted, the shear modulus was 80 GPa, and the density was 7850 kg/m^3 [3–10]. The standard metallographic procedure was performed after sectioning the samples in the direction parallel to the motion direction. After cutting, the sample was poured into resin, polished with silicon carbide sandpaper (grain size 1200–3000) and polished with 0.5 μm microsilica. The cross section was observed under an optical microscope after etching with a 2% alcohol solution of nitric acid for 7 seconds. The mechanism of a white layer formation was investigated through the *SYSWELD* program, which uses an analytical model of the volumetric heat release of Goldak double ellipsoid. Three types of heat source are prescribed: 2D Gaussian, double ellipsoid and 3D conical Gaussian. After the geometric parameters of the heating model are determined and the maximum volumetric heat release value is set, an approximate calculation with constant thermophysical characteristics is performed. All material properties necessary for modeling are set in the form of piecewise linear functions. In the *SYSWELD* program, simultaneously with the heat problem, the metallurgical problem is solved. In the latter case, the calculations are based on the Leblond model, which describes the metallurgical transformation of one phase into another. The solution to the mechanics problems is reduced to the determination of thermal deformations. To do this,

you need to specify in the program the following: elasticity modulus, Poisson's ratio, thermal-expansion coefficient, as well as hardening curves for metallurgical phases. When cracking in a white layer under the moving contact conditions, observations were performed using ANSYS/LS-DYNA software, which is intended for finite element modeling. In studies on the dynamics of railway crews, the well-known algorithm of the named software *FASTSIM* with an elliptical contact area is widely used [25]. Compared with the geometric dimensions of the wheel and rail, the contact area is quite small (not more than 15 mm^2 [25]). Therefore, the model of wheel – rail contact can be simplified to the condition of deformation of the 2D plane [26, 27]. White layers in the form of an arc 2 mm long and 0.2 mm thick were constructed on the longitudinal section (the parameters were obtained as a result of the analysis of *WEL* studies on the rail surface [4–15]). In order to reduce computational costs and ensure accuracy in the model, the adaptive grid method was used. In the region of the white layer, very fine grids were used (Fig.1).

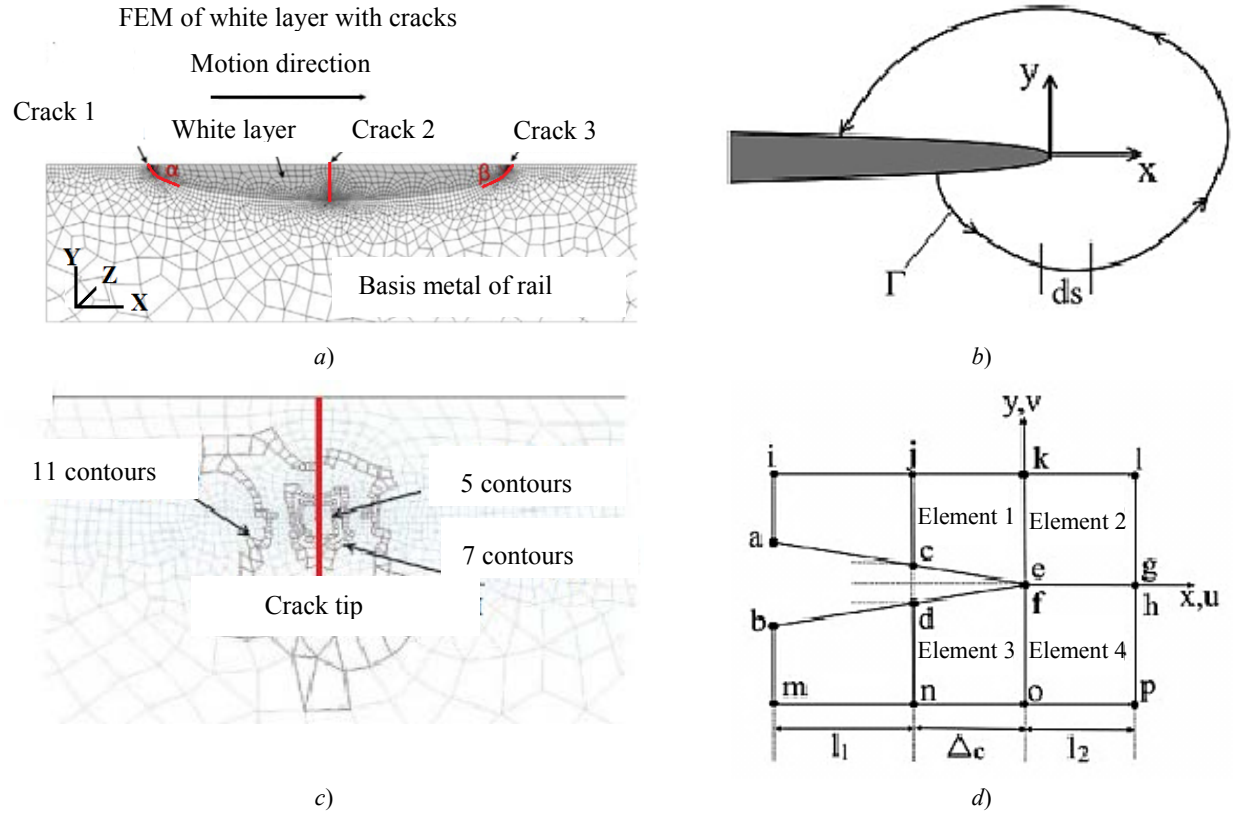

Fig. 1. Finite element modeling (FEM) of white layer with three cracks (a) and transformation of element contour integral into surface contour integral: arbitrary contour around the crack tip (b); different contours of elements selected to represent independence from the calculation path of J-integral (c); basic diagram of 2D virtual crack closure method for calculating stress intensity factor (d)

The established minimum element size was 0.02×0.02 mm^2. The elements had a higher grid density with a set minimum element size of 0.01×0.01 mm^2 at the tips and faces of cracks. This enabled to accurately capture the stress gradients. Outside the cracking zone, larger grids were used with a minimum element size of 0.1×0.1 mm^2 in the wheel – rail contact surfaces. They gradually increased towards the far sections of the field. At first, the rail was combined into 776,919 elements with 789,084 nodes, which changed during the simulation due to the use of the adaptive grid method. Such a model size is acceptable for obtaining accurate calculations of contact with rolling [19, 20, 28]. A constant vertical loading force of 13,000 N was applied to the wheel, which corresponded to the equivalent maximum Hertz pressure of ~ 1.2 GPa [25]. The wheel was set to a rotation speed of ω 43.5 rad/s, which equals a travel speed of 72 km/h with a friction coefficient of 0.3. It was studied how the properties of cracks in a white layer are affected by their length, changes in the angle of inclination, load pressure, and friction coefficient.

The crack growth that destroys the surface was analyzed under the assumption of linear elastic fracture mechanics [1–3, 17–19]. For a more accurate solution, we used the criterion of elastic-plastic fracture mechanics, the *J*-integral method, which is applicable for both linear and elastic plastic solutions [29]. It was introduced to study crack propagation behavior. For numerical calculations, the *J*-integral can be obtained from the solution in the far zone [29]. In the scope of work with finite elements, the element contour integral should be transformed into the surface contour integral, as shown in Fig. 1*b*, where Γ is the contour of the curve that defines the boundary of the *J*-integral, and it is directed counterclockwise from the lower edge of the crack to the upper one. The *J*-integral can be additionally estimated as:

$$J = \int (w\,dy - T_i \frac{du_i}{dx} ds),$$

where w is strain energy density; T_i is the thrust vector; u_i is the component of the displacement vector; ds is the length increment along the contour Γ [29].

The *J*-integral evaluation is implemented in *LS-PrePost* as a post-processing tool. This application is also suitable for 2D modeling of plane deformation [30]. To calculate the *J*-integral around the crack tip, various contours of the elements were selected (see Fig. 1*c*). It is important to note that the unloading conditions for a path-independent *J*-integral are not proposed in accordance with the fracture mechanics [31]. The principle of expanding the *J*-integral methodology beyond the admissibility of linear elastic fracture mechanics was to idealize elastoplastic deformation as a nonlinear elastic deformation. The identity of the load characteristics — the deformation for elastoplastic and nonlinear elastic materials is known [30, 31]. The elastic-plastic material follows a linear unloading path with a slope equal to Young's modulus. Non-linear elastic material gets unloaded in the same way as when loading. Thus, the analysis suggests that the nonlinear-elastic behavior is valid for an elastoplastic material. Unloading occurs near the crack tip after the wheel has passed along the rail. The calculated values of the *J*-integral can be valid only until maximum is reached. Therefore, only the maximum values of the *J*-integral are discussed in the present paper. The stress intensity factors within the framework of the finite element scheme were calculated by the 2D method of virtual crack closure [29–32]. The forces *y* and *x* needed to connect the nodes *c* and *d* (see Fig. 1*d*) are denoted by F_c and T_c, respectively.

It should be noted that the theory of linear elastic fracture mechanics is based on the assumption that there is no plastic deformation around the cracks. At the same time, according to [1–3], the use of the theory of linear elastic fracture mechanics is correct since the nonlinear deformation of the material is limited to a small area surrounding the crack tip. The reasoning that a plane problem can be considered in connection with a small contact area is incorrect. Under the plane deformation, this region is strip and infinite. And in this case, we are talking about an essentially three-dimensional problem. In [32], the complexity of the rail geometry and the boundedness of the region in which the main changes in the stress-strain state occur. The authors of this paper propose to consider a simplified axisymmetric problem for a multilayer coating in the form of a piecewise inhomogeneous layer. In [33], the stress-strain state of a multilayer coating was studied in the vicinity of the wheel – rail contact area. It was shown that the rigidity and thickness of the upper coating layer affect significantly the equivalent and contact stresses. At the fixed mechanical parameters of the coating, with an increase in the thickness of its upper layer, the values of maximum equivalent and contact stresses decrease. The authors of [34] applied thin multilayer coatings on the surface of a railway rail in the vicinity of the lateral wheel – rail contact. The stress-strain state of these coatings was investigated at various values of their geometric and mechanical parameters during rotary movements.

Research Results. Fig. 2 shows optical images of the microstructure of the cross section of a white layer on the rail surface.

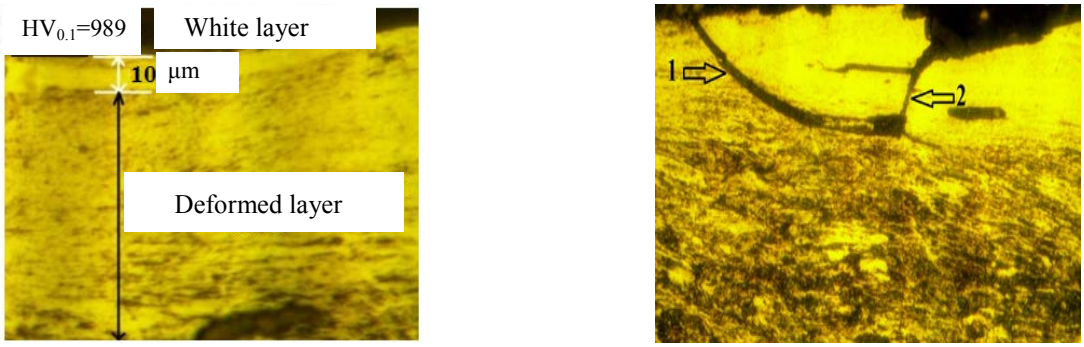

a) *b*)

Fig. 2. Features of cracks in white layer on rail surface detected through optical microscopy: general view of white and deformed layer at 200-fold magnification (*a*); 1 - front edge crack, 2 - mid-position crack at 500x magnification (*b*)

Fig. 2*a* shows a segment of a white layer on the surface. Its depth is 10 μm. The microhardness value in the white layer is $HV_{0.1}$ = 989. This corresponds to the *WEL* features presented in [4–15]. The *WEL* thickness can reach 200–300 μm depending on the operating conditions [4–6]. The image shows a sharp boundary between the white layer and the deformed pearlite structure of the basis rail metal. The depth of the plastic deformation zone between *WEL* and the basic rail material is ~ 70 μm. According to the estimates [5–10], on the pearlitic rails in operation, in the spot of the wheel – rail contact, plastic deformation has a high concentration creating a thin shear zone of 502,180 μm. At the same time, hardness tests show that due to volume contact, the depth of plastic deformation can reach 1–10 mm [4–9, 27–30]. This causes an important evolution of the microstructure on a narrower scale, i.e., to bend or rupture of cementite plates, to reduction of the inter-plate distance. The mechanical properties also change since the tensile strength increases and the fracture toughness decreases for cracks parallel to the aligned cementite plates. Two different cracks are located at the leading edge of the *WEL* (see Fig. 2*b*). They can originate and propagate at the interface between the *WEL* and the deformed pearlite microstructure. A detailed study on other samples showed that an inclined crack appeared on the leading edge of the *WEL* following the flow direction of the rail material. Then the crack went down into the rail material along the layer boundary. Fig. 2*b* shows a crack propagating vertically in the mid-position within the *WEL*. In the samples studied, two different types of cracks are observed at the trailing edge of the *WEL*. They are obtained from different *WEL* sections, but are located on the same rail sample and are very close to each other. The first-type crack originates and propagates along the boundary between the white layer and the plastic deformation zone (see Fig. 2*b*). The second-type crack crosses the interface with a deformed microstructure, but shows a tendency to curvature along the line in the direction of perlite shear strain. Such behavior of cracks is described in [4–7]. Indeed, the cracks studied by us are located in the same white layer; therefore, they were subjected to the same loads. However, their growth and development rates are different. This indicates a change in the state of stress in the leading, middle and rear position in the white layer. This means that the mechanism for the subsequent crack propagation (i.e., behind it) should be different. As shown in [35, 36], the plastically deformed structure of the pearlite region directly below the white layer can play a significant role in effecting the crack propagation. Cracks that are formed due to fatigue when in the rolling contact can be divided into two categories according to the place of their origination: beneath the surface and on the surface.

Typically, cracks beneath the surface result from a strong vertical load in conjunction with material defects. Most cracks originate on the surface due to the wheel – rail interaction, as well as the transfer of a large load to a small contact area. The contact area is elliptical. It is relatively small, and at the same time, it supports the entire wheel load. Cracks, that arise as a result of fatigue when in the rolling contact and are the result of intense shear stress in the wheel – rail contact area, will grow when these stresses exceed the allowable tensile strength of the rail. It is also possible that cracks will advance to the top of the rails. According to [11, 12, 23], the heating rate of the surface layer of the rail,

which occurs during the passing of a train, can exceed 10^6°C/s and reach the temperature at which austenite is formed. After passing the train under rapid cooling, austenite turns into martensite. The wheel – rail contact time is extremely short (milliseconds). In this case, the steel of the eutectoid composition is heated from room temperature to 727°C at a rate of 10^6°C/s.

Thus, it is practically impossible to measure actual temperature changes during the period under consideration. On the other hand, fast heating and hardening can be modeled and controlled in the *SYSWELD* program. For this, heating rates of 20–1000°C/s were used, which were obtained due to the parameter of the velocity of the heat source moving along the rail surface in the speed range 5–100 mm/s.

Fig. 3 shows a fragment of modeling the mechanism of formation of a white layer in the *SYSWELD* program.

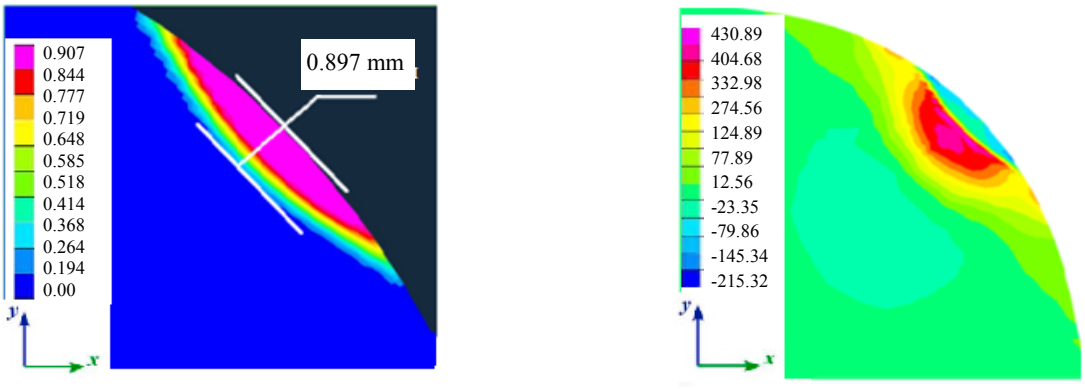

a) *b*)

Fig. 3. Simulation results of white layer formation on the rail head surface in SYSWELD program: martensite fraction in the white layer, % (a); distribution of residual stresses in the white layer, MPa (b).

According to Table 1, we can judge how the level of residual stresses depends on the parameters of the path and the hardening rate.

Table 1

Residual stresses value (compression and tension) along the path width and depth at a hardening speed of 15 mm

Distance along the center of the path axis (depth), mm	0	0.65	0.77	0.86	0.96	1.22	1.54	2.5	3.0
Residual stress, MPa	–43	–87	–15	323	445	347	396	274	176
Centre distance from path axis (width), mm	0	0.14	1.65	1.92	2.19	2.59	3.16	3.91	5.2
Residual stress, MPa	–43	–92	–140	–189	–116	30	200	249	128

The white layer modeled in the program consists of martensite. The layer morphology is similar to that observed in the studied rail (see Fig. 2). The hardness of the simulated *WEL* is 670–810 *HV*. This is slightly lower than in rails (*WEL* ~ 725–1050 *HV*). However, current simulations represent only one phase transformation cycle. From one to five repeated heat treatment cycles were simulated on the surface of the rail head. It is found that hardness increases to 700–850 *HV*. Obviously, martensite with the same hardness as in the white layer of the rail can be obtained after several passes of the wheels. When modeling the formation of the white layer, it turned out that the temperature change during the wheel – rail contact and the distribution of residual stresses play an important role in this process.

Fig. 4 shows *J*-integral maxima at the tips of the simulated crack.

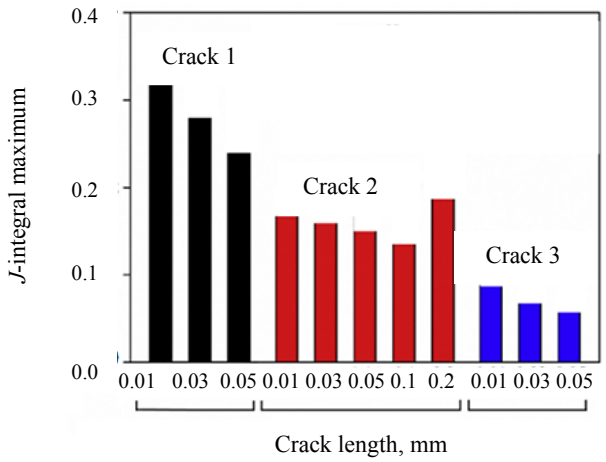

Fig. 4. Maximum values of *J*-integral at crack tips in the leading, middle, and trailing edges of *WEL* (crack length for calculation is chosen as 0.01 mm; 0.03 mm; 0.05 mm; 0.1 mm and 0.2 mm, separately)

It should be noted that the length of the crack is measured from the rail surface to the *WEL* depth. In the presented simulation version, cracks no. 1, 3 originate at an angle α and β (83.13°), the maximum load pressure is 1.2 GPa. At this, all three cracks have a length of 10 μm. At the top of crack no. 1, the value of the *J*-integral reaches a maximum of 0.321 N/mm. The maximum values of the *J*-integral for cracks nos. 2 and 3 are much smaller — 0.18 N/mm and 0.088 N/mm, respectively. The analysis of Fig. 4 shows that crack no. 1 at the leading edge of *WEL* is likely to grow compared to cracks in the mid-position and at the trailing edge. This fact is in agreement with rolling fatigue experiments [10–18]. It is shown that the boundary (beginning) of the white layer on the rail surface and the basis metal has the lowest resistance to the formation of a contact-fatigue defect, while the fatigue life at the end of the *WEL* is approximately 3 times higher than in the center and at the starting point. Fig. 4 shows that the maxima of the *J*-integral around the crack tips show a tendency to decrease with increasing length or depth. This phenomenon is more significant for crack no. 1 than for nos. 2 and 3. As the crack length increases, the maximum value of the *J*-integral for all three cracks decreases, respectively, from 0.3214 *N*/mm to 0.222 *N*/mm; from 0.18 *N*/mm to 0.14 *N*/mm and from 0.088 *N*/mm to 0.062 *N*/mm. This is consistent with the results of [19] since the deeper surfaces of the crack are less affected by normal and tangential contact loads. However, Fig. 4 shows that, for crack no. 2, when its length is 200 μm and corresponds to the *WEL* thickness, the *J*-integral maximum tends to the opposite, which has never been reported. In this case, the *J*-integral maximum is the largest in comparison with other short cracks no. 2. It can be assumed that crack no. 2 will rapidly propagate to the boundary between the *WEL* and the substrate. This is clearly seen in Fig. 2*b* (arrow 2). The significant difference is due to material irregularities between the perfectly elastic *WEL* and the elastic-plastic rail matrix. The calculation results show that for all three cracks the values of the J-integral decrease slightly when the crack length increases from 10 to 50 μm. If the deepening of crack No. 2 is from 50 to 100 μm, the change in the J-integral is relatively small. On the contrary, there is a significant increase in the maximum value of the J-integral if crack No. 2 propagates through the entire layer to the boundary between WEL and the rail matrix. The calculation results show that for all three cracks, the values of the *J*-integral decrease slightly when the crack length increases from 10 to 50 μm. If the deepening of crack no. 2 is from 50 to 100 μm, the change in the *J*-integral is relatively small. On the contrary, there is a significant increase in the maximum value of the *J*-integral if crack no. 2 propagates through the entire layer to the boundary between the *WEL* and the rail matrix.

The maximum value of the *J*-integral increases sharply with increasing load pressure from 0.8 to 1.5 GPa:

- from 0.27 N/mm to 0.53 N/mm for crack no. 1;
- from 0.17 N/mm to 0.47 N/mm for crack no. 2;
- from 0.04 N/mm to 0.1 N/mm for crack no. 3.

This suggests that cracks are more likely to propagate at high loads. The maximum principal stress around the crack tip can be used as an indicator to assess the fracture properties and the crack path [19–26]. For example, if no. 1 crack length is 10 μm, the maximum principal stress at the crack tip is 1589 MPa. For cracks nos. 2 and 3 with the same length, different stress concentrations are obtained around the crack tips and the maximum principal stresses are about 1506 MPa and 1261 MPa, respectively. An increase in length from 10 to 100 μm causes a decrease in the maximum principal stress from 1506 MPa to 1206 MPa. When a crack propagates down to the boundary of the white layer, a sharp increase in stress concentration can be observed. This is clearly seen from modeling the distribution of residual stresses along the depth of the layer (see Fig. 3). So, according to *J*-integral calculations, under the same load conditions, cracks in the leading edge of the white layer propagate with greater probability than in the mid-position and at the trailing edge. This is consistent with crack growth. In this case, due to the inhomogeneity of the material, a complex stress field arises when the middle crack propagates at the interface between the white layer and the base metal. This causes a high concentration of stresses and thereby accelerates the crack propagation. It should be mentioned that this work did not consider the anisotropic characteristics of the material caused by severe plastic deformation in the transition zone. It was shown in [4–10] that this type of shear deformation causes elongation and alignment of cementite colonies of the surface layer of the rail head (see Fig. 2*a*). It is revealed that shear bands and regions with a high density of defects are found in the transition zone of the white layer, and some cementite plates in this region are destroyed [4–8]. Although linear elastic fracture mechanics does not reflect the detailed physics of the situation [1-3], it helps to understand the directions of the observed crack growth. To obtain more detailed information on the dynamics of crack formation in the white layer on the rail surface, stress intensity factors should be taken into account. At the same time, rolling contact cracks experience a mixed load corresponding to a sequence of tensile stresses followed by a shear cycle [4–20]. Therefore, stress intensity factors in the direction of maximum tangential stress can also be used to predict the direction of the crack growth.

Discussion and Conclusions. It is established that cracks in the leading edge of the white layer (crack no. 1) propagate from the edge of the layer along the interface between the white layer and the basis metal of the rail. Cracks no. 2 (in the middle of the layer) grow vertically before reaching the plastically deformed matrix. Cracks no. 3 of the trailing edge show two developmental trends. In the first case, the crack extends along the interface; in the second case, it crosses the rail material and gradually aligns in the direction of deformation.

Comparisons of the *J*-integral maxima have shown that under identical load conditions, crack no. 1 is most likely to have a high growth rate compared to cracks nos. 2 and 3. With an increase in the crack length, the maxima of the *J*-integral of all three cracks decreased. A great impact of the load pressure on the development of all the considered types of cracks is established.

References

1. Kogaev VP, Makhutov NA, Gusenkov AP. Raschety detalei mashin i konstruktsii na prochnost' i dolgovechnost' [Calculations of machine parts and structures for strength and durability]. Moscow: Mashinostroenie; 1985. 224 p. (In Russ.)

2. Broek D. Osnovy mekhaniki razrusheniya [Fundamentals of Fracture Mechanics]. Moscow: Nauka; 1974. 288 p. (In Russ.)

3. Vitvitskii PM, Popina SYu. Prochnost' i kriterii khrupkogo razrusheniya stokhasticheski defektnykh tel [Strength and criteria for brittle fracture of stochastically defective bodies]. Kiev: Naukova dumka; 1980. 186 p. (In Russ.)

4. Clayton P, Allery MBP. Metallurgical aspects of surface damage problems in rails. The Canadian Journal of Metallurgy and Materials Science. 1982;21(1):31–46.

5. Baumann G, Fecht H, Liebelt S. Formation of White-Etching Layers on Rail Treads. Wear. 1996;191:133–140. doi.org/10.1016/0043-1648(95)06733-7.

6. Newcom SB, Stobbs WM. A transmission electron microscopy study of the white etching layer on a railhead. Materials Science and Engineering. A. 1984;66(2):195–204. doi.org/10.1016/0025-5416(84)90180-0.

7. Jirásková Y, Svoboda J, Schneeweiss O, et al. Microscopic investigation of surface layers on rails. Applied Surface Science. 2005;239(2):132–141. doi.org/10.1016/j.apsusc.2004.05.289.

8. Österle W, Rooch H, Pyzalla A, et al. Investigation of white etching layers on rails by optical microscopy, electron microscopy, X-ray and synchrotron X-ray diffraction. Materials Science and Engineering. A. 2001;303(1/2):150–157.

9. Lojkowski W, Djahanbakhsh M, Bürkle G, et al. Nanostructure formation on the surface of railway tracks. Materials Science and Engineering. A. 2001;303(1/2):197–208. doi.org/10.1016/S0921-5093(00)01947-X.

10. Zhang HW, Ohsaki S, Mitao S, et al. Microstructural investigation of white etching layer on pearlite steel rail. Materials Science and Engineering. A. 2006;421(1/2):191–199. doi.org/10.1016/j.msea.2006.01.033.

11. Chou YK, Evans CJ. White layers and thermal modeling of hard turned surfaces. International Journal of Machine Tools and Manufacture. 1999;39(12):1863–1881. doi.org/10.1016/S0890-6955(99)00036-X.

12. Clayton P. The relations between wear behavior and basic material properties for pearlitic steels. Wear. 1980;60(1):75–93.

13. Steenbergen M, Dollevoet R. On the mechanism of squat formation on train rails. Part II: growth. International Journal of Fatigue. 2013;47:373–381.

14. Li Z, Dollevoet R, Molodova M, et al. Squat growth — some observations and the validation of numerical predictions. Wear. 2013;271(1):148–157. doi.org/10.1016/j.wear.2010.10.051.

15. Olzak M, Stupnicki J, Wojcik R. Investigation of crack propagation during contact by a finite element method. Wear. 1991;146(3):119–128.

16. Bold PE, Brown MW, Allen RJ. Shear mode crack growth and rolling contact fatigue. Wear. 1991;144(1/2):307–317.

17. Ringsberg JW. Shear mode growth of short surface-breaking RCF cracks. Wear. 2005;258(7):955–963.

18. Seo J, Kwon S, Jun H, et al. Fatigue crack growth behavior of surface crack in rails. Procedia Engineering. 2010;2(1):865–872. doi.org/10.1016/j.proeng.2010.03.093.

19. Xin Zhao, Xiaogang Zhao, Chao Liu, et al. A study on dynamic stress intensity factors of rail cracks at high speeds by a 3D explicit finite element model of rolling contact. Wear. 2016;366–367:60–70 /doi.org/10.1016/j.wear.2016.06.001.

20. Trollé B, Baietto M-C, Gravouila A, et al. 2D fatigue crack propagation in rails taking into account actual plastic stresses. Engineering Fracture Mechanics. 2014;123:163–181. doi.org/10.1016/j.engfracmech.2014.03.020.

21. Bogdański S, Lewicki P. Experimental and theoretical investigation of the phenomenon of filling the RCF crack with liquid. Wear. 2005;258(7-8):1280–1287. doi.org/10.1016/j.wear.2004.03.038.

22. Makino T, Kato T, Hirakawa K . The effect of slip ratio on the rolling contact fatigue property of railway wheel steel. International Journal of Fatigue. 2012;36(1):68–79. doi.org/10.1016/j.ijfatigue.2011.08.014.

23. Dubourg MC, Lamacq V. A predictive rolling contact fatigue crack growth model: onset of branching, direction, and growth — role of dry and lubricated conditions on crack patterns. Journal of Tribology — Transactions of the ASME. 2002;124(4):680–688. DOI: 10.1115 / 1.1479698.

24. Benuzzi D, Bormetti E, Donzella G. Stress intensity factor range and propagation mode of surface cracks under rolling — sliding contact. Theoretical and Applied Fracture Mechanics. 2003;40(1):55–74. doi.org/10.1016/S0167-8442(03)00034-X.

25. Kalker JJ, Piotrowski J. Some New Results in Rolling Contact. Vehicle System Dynamics. 1989;18:223–242. doi.org/10.1080/00423118908968920.

26. Kato T, Sugeta A, Nakayama E. Investigation of influence of white layer geometry on spalling property in railway wheel steel. Wear. 2011;271(1):400–407. doi.org/10.1016/j.wear.2010.10.024.

27. Seo JW, Kwon S, Jun HK, et al. Numerical stress analysis and rolling contact fatigue of White Etching Layer on rail steel. International Journal of Fatigue. 2011;33(2):203–211. doi.org/10.1016/j.ijfatigue.2010.08.007.

28. Lian Q, Deng G, Juboori AA, et al. Crack propagation behavior in white etching layer on rail steel surface. Engineering Failure Analysis. 2019;104:816–829. doi.org/10.1016/j.engfailanal.2019.06.067.

29. Rice JR. A Path Independent Integral and Approximate Analysis of Strain Concentration by Notches and Cracks. Journal Applied Mechanics. 1968;35:379–386.

30. Rybicki EF, Kanninen MF. A finite element calculation of stress intensity factors by a modified crack closure integral. Engineering Fracture Mechanics. 1977;9(4):931–938. doi.org/10.1016/0013-7944(77)90013-3.

31. Chow WT, Atluri SN. Finite element calculation of stress intensity factors for interfacial crack using virtual crack closure integral. Computational Mechanics. 1995;16:417–425. https://doi.org/10.1007/BF00370563.

32. Danil'chenko SA, Nasedkin AV. Modelirovanie uprugogo indentirovaniya mnogosloinogo antifriktsionnogo pokrytiya rel'sa metodom konechnykh ehlementov [Modeling of elastic indentation of multilayer antifriction rail coating by the finite element method]. Izvestia RAS SamSC. 2011;13(3):1029–1032. (In Russ.)

33. Chebakov MI, Kolosova EM, Nasedkin AV. Modelirovanie kontaktnogo vzaimodeistviya tel s neodnorodnymi po glubine mekhanicheskimi svoistvami pri nalichii treniya v zone kontakta [Modeling of contact interaction of bodies with mechanical properties non-uniform in depth in the presence of friction in the contact zone]. Izvestia RAS SamSC. 2011;13(4):1252–1255. (In Russ.)

34. Nasedkin AV, Sukhov DYu, Chebakov MI. Modelirovanie kontaktnogo vzaimodeistviya zheleznodorozhnogo kolesa i rel'sa s tonkim trekhsloinym pokrytiem [Modeling of contact interaction between wheel and rail with thin triple-layered covering]. Vestnik RGUPS. 2010;2:11–16. (In Russ.)

35. Al-Juboori A, Wexlera D, Lia H, et al. Squat formation and the occurrence of two distinct classes of white etching layer on the surface of rail steel. International Journal of Fatigue. 2017;104:52–60. doi.org/10.1016/j.ijfatigue.2017.07.005.

36. Li S, Wu J, Petrov RH, et al. Brown etching layer: a possible new insight into the crack initiation of rolling contact fatigue in rail steels. Engineering Failure Analysis. 2016;66:8–18. doi.org/10.1016/j.engfailanal.2016.03.019.

Submitted 21.03.2020
Scheduled in the issue 20.04.2020

About the authors:

Perelygina, Aleksandra Yu., acting head of the Engineering and Computer Graphics Department, Irkutsk National Research Technical University (83, Lermontov St., Irkutsk, 664074, RF), Cand.Sci. (Eng.), ResearcherID AAF-1094-2020, ORCID: https://orcid.org/0000-0001-7814-0431, perelygina@isru.edu

Konyukhov, Vladimir Yu., professor of the Automation and Management Department, Irkutsk National Research Technical University (83, Lermontov St., Irkutsk, 664074, RF), Cand.Sci. (Eng), professor, ResearcherID AAE-5296-2020, ScopusID 56769690400, ORCID: https://orcid.org/0000-0001-9137-9404, c12@ex.istu.edu

Balanovskii, Andrei E., associate professor of the Engineering Technologies and Materials Department Irkutsk National Research Technical University (83, Lermontov St., Irkutsk, 664074, RF), Cand.Sci. (Eng.), ResearcherID AAE-2964-2020, ScopusID 56375902200, ORCID: https://orcid.org/0000-0002-6466-6587, fuco.64@mail.ru

Claimed contributorship

A.Yu. Perelygina: literature analysis; research objective selection; task setting; planning and organization of joint work; development of a model of cracking in a white layer under conditions of moving contact using commercial *ANSYS / LS-DYNA* finite element modeling software; the paper writing. V. Yu. Konyukhov: the calculated data analysis; parametric identification of models based on graphical experimental distributions using statistical methods and *Excel* spreadsheets. A. E. Balanovskii: experimental work on materials science (cutting, testing, preparation, metallography, measuring the hardness of samples of rails with a white layer); development of a model for the formation of a white layer on the rail head using the *SYSWELD* program; the paper writing.

All authors have read and approved the final manuscript.